ОСОБЕННОСТИ ГАЗОНАКОПЛЕНИЯ В МЕНЕЕ ПРОДУКТИВНЫХ НИЗКОПРОНИЦАЕМЫХ КОЛЛЕКТОРАХ ИНТЕРВАЛА НЕ 8 НА ГАЗОВОМ МЕСТОРОЖДЕНИИ СУЛИГЭ (*Ордосский бассейн, Китай*)

Дин Сяоци[1], Ян Пэн[2,3], Хань Мэймэй[3], Чэнь Ян[3,4], Чжан Сыян[5], Чжан Шаонань[2], Лю Сюйань[1], Гун Имин[1], А.М. Нечваль[4]

[1] *State Key Laboratory of Oil and Gas Reservoir Geology and Exploitation, Chengdu University of Technology, Sichuan 610059, China*

[2] *Northwest Petroleum Bureau of Sinopec, Xinjiang 830011, China*

[3] *State Key Laboratory of Oil and Gas Reservoir Geology and Exploitation, Southwest Petroleum University, Sichuan 610500, China*

[4] *Teaching and Research Office of Oil and Gas Engineering, Ufa State Petroleum Technological University, Ufa, 450062, Russian*

[5] *Department of Geology, University of Regina, Regina s4s 3x3, Canada*

Ввиду недостаточной обеспеченности природным газом из материнских пород, а также потерь газа, среди газовых коллекторов Китая значительную долю составляют менее продуктивные месторождения газа плотных пород. Эти месторождения малочисленны, однако обладают большими запасами. На примере низкопроницаемых коллекторов Не 8 в западной части газового месторождения Сулигэ изучено распределение газа при менее продуктивном газонакоплении. Согласно результатам исследования, во-первых, поступление газа в значительной мере зависит от уплотнения песчаника. Уплотнение литаренита к моменту масштабного заполнения газом уже завершено, что не может способствовать лучшему протеканию процесса. Напротив, в случае сублитаренита, несмотря на то, что он испытал сильное уплотнение до образования газа, обрастание кварцем, приводящее к дальнейшему уплотнению пород-коллекторов, проходит одновременно с крупномасштабным поступлением газа. Это облегчает газонакопление, сопровождаемое уплотнением пород и формированием коллекторов. Во-вторых, газонакопление может в некоторой степени контролироваться локальной структурой. В частности, при определённых физических свойствах песчаников локальной структуры газонасыщение может увеличиться приблизительно на 7 %. В-третьих, менее продуктивное заполнение газом является основной причиной сложноструктурированного распределения газа и воды в коллекторах Не 8. Дополнительные факторы — сильная неоднородность коллекторов и понижение давления в них за счёт тектонического поднятия в яньшаньский период. В результате из коллекторов Не 8 образовалось многоколлекторное месторождение с несколькими газоводяными контактами. Коллекторы Не 8 не являются традиционными либо низкопроницаемыми. Более вероятно, что они квазинизкопроницаемы и накопление газа контролируется как верхним слоем песчаников, так и физическими свойствами пород-коллекторов. Литологические ловушки и высококачественные коллекторы в локальных ловушках благоприятствуют газонакоплению.

Газ плотных пород, распределение газа и воды, коллектор, неоднородность, интервал Не 8, *газовое месторождение Сулигэ, Ордосский бассейн.*

CHARACTERISTICS OF GAS ACCUMULATION IN A LESS EFFICIENT TIGHT-GAS RESERVOIR, HE 8 INTERVAL, SULIGE GAS FIELD, ORDOS BASIN, CHINA

Ding Xiaoqi, Yang Peng, Han Meimei, Chen Yang, Zhang Siyang, Zhang Shaonan, Liu Xuan, Gong Yiming, and A.M. Nechval

Abstract: Because of the lack of gas supply from source rocks and gas loss, inefficient tight-gas fields represent a high share of all gas reservoirs in China. These gas fields are characterized by low abundance and large gas reserves. Here, the He 8 tight-gas reservoirs in the western region of the Sulige gas field are used as an example to characterize gas distribution under conditions of less efficient charging. Results show the following characteristics. First, the sandstone densification process has a relatively large impact on the charging of gas. Litharenite was already subjected to densification at the time of large-scale gas charging, and this was not conducive to gas charging. On the contrary, for sublitharenite, although strong compaction has already occurred during gas generation, quartz overgrowth that leads to further densification of the gas reservoirs occurs simultaneously with large-scale gas charging. This facilitates gas charging, and is characterized by concomitant densification and reservoir formation. Second, structure traps can control the accumulation of gas to a certain extent. In particular, when physical properties of sandstones within the structure traps are appropriate, gas saturation during gas charging can be increased by approximately 7%. Third, less efficient charging is the main cause of the complex gas and water distribution in the He 8 gas reservoirs. The strong heterogeneity of the reservoirs and the decline in the gas reservoir pressure caused by tectonic uplift in the Yanshan period further exacerbate the complexity of gas and water distribution. These factors ultimately caused the He 8 gas reservoirs to become

a multireservoir gas field with several gas–water interfaces. He 8 gas reservoirs are neither conventional gas nor continuous gas reservoirs. Rather, they are quasi-continuous gas reservoirs, and the accumulation of gas is controlled by both the top surface of sandstone and physical properties of the reservoirs. Traps and high-quality reservoirs within the regional traps are beneficial for the gas accumulation.

INTRODUCTION

Tight gas is also known as deep basin gas, basin-center gas or continuous gas. Having this variety of names, this unconventional gas will be the focus of exploration and development programs for a considerably long time in the future because of vast amount of accessible gas in the deposits (Meckel and Thomasson, 2008). Different countries and institutions have different standards with respect to definition of tight-gas sandstones. In the United States, sandstones with surface permeability of less than 0.1 md are defined as tight sandstones. In Canada, a cutoff of 1.0 md is commonly used. However, in China, the cutoff is 0.1 md under overburden pressure (Zou et al., 2013).

Camp (2011) and Shanley et al. (2004) summarized the general characteristics of tight-gas sandstones as: 1) extensive gas shows while drilling; 2) little produced water; 3) low permeability of reservoirs, generally less than 0.1 md; 4) abnormal pressure, but subnormal generally; 5) poorly defined traps and seals; 6) proximity to mature source rocks, and 7) no gas-water contacts. Buoyancy is minimal or nonexistent in gas accumulation because of no water contacts and extensive gas shows. So, this is the fundamental difference compared to conventional gas (Nelson, 2009; Law and Curtis, 2002). It is believed that tight-gas reservoirs can't produce water or produce little water because there is no relationship between gas accumulation and traps. But with the subsequent exploration and development, producing water in gas wells is pervasive (Camp, 2011). Wells in the Uintah, Piceance and Great River basins reveal that 70-80% of the wells have water/gas ratios exceeding 1.0 bbl/mmcf, greater than that expected from gas condensation (Cumella et al. 2008).

Pervasive tight-gas sandstones may appear in any basin and at any position in the basin, but the commonality is that it is located close to the mature source rocks (Law, 2002; Meckel and Thomasson, 2008; Shanley et al., 2004; Schmoker, 2002). Gas accumulation is controlled by many factors, often associated with pressure, reservoir quality, fractures and subtle traps (Bates et al., 2001; Hirst and Davis, 2001). Li et al. (2012) and He (2003) stated that presently, most of the tight-gas reservoirs are related to coal-bearing strata, such as Cretaceous gas reservoirs in San Juan Basin in the Midwest U.S., Cretaceous reservoirs in Green River Basin in U.S., Upper Paleozoic gas reservoirs in Ordos Basin, and Triassic Xujiahe gas reservoirs in Sichuan Basin in China (Dai, 2014; Hood and Yurewicz, 2008; Yang et al., 2007; Zou et al., 2009). Based on the quality of gas charging, tight-gas reservoirs can be divided into two types (Meckel and Thomasson, 2008): efficient charging and less efficient charging. When the charging is adequate and efficient, there is no down dip gas-water contact and water free production. Where the charging is less efficient, gas reservoirs have a small amount of residual water pockets because the displacement of pore water by gas is not complete in tight-gas sandstone reservoirs. In the late stage of development, producing water is seen to varying degrees. If the charging quality is relatively high in a less efficient charging gas reservoir, residual water will be diffused in the tight-gas reservoirs, and no obvious edge or bottom water is formed. If the charging quality is relatively low, diffused free water exists in the tight-gas reservoirs in addition to the appearance of notable edge and bottom water (Meckel and Thomasson, 2008). Less efficient tight-gas reservoirs dominate on the territory of China. These types of gas reservoirs are characterized by low abundance and large reserves. A priority task in future exploration and development of unconventional tight-gas reservoirs is how to use this part of the materials from gas reserves (Zhao et al., 2005).

In this paper the He 8 tight-gas reservoirs from the western region of the Sulige gas field are used to examine the basic elements of gas accumulation, and to discuss factors controlling gas accumulation, in order to provide a geological basis for the next development.

The Sulige gas field is located in the northwest of the Yishan Slope (Figure 1), with an exploration area of approximately 4×10^4 km². The main gas production layers include the Permian He 8 member of the Shihezi Formation and the Shan 1 member of the Shanxi Formation (Figure 2). Sulige is Chinas's largest onshore gas reserve with the highest gas yield. It was discovered in 2000, with proved reserves totaling 2.85×10^{12} m³ (Yang et al., 2012). In 2013, the gas yield exceeded 210×10^8 m³.

The He 8 sandstone in the western region of Sulige is tight. Its average porosity is 8.5%, with a permeability of 0.997 md and overburden pressure permeability of 0.042 md, making it a typical tight-gas sandstone reservoir. Hydrocarbon-generating intensity in the west of Sulige is $10\text{-}15 \times 10^8$ m³/km², which is a lot less than
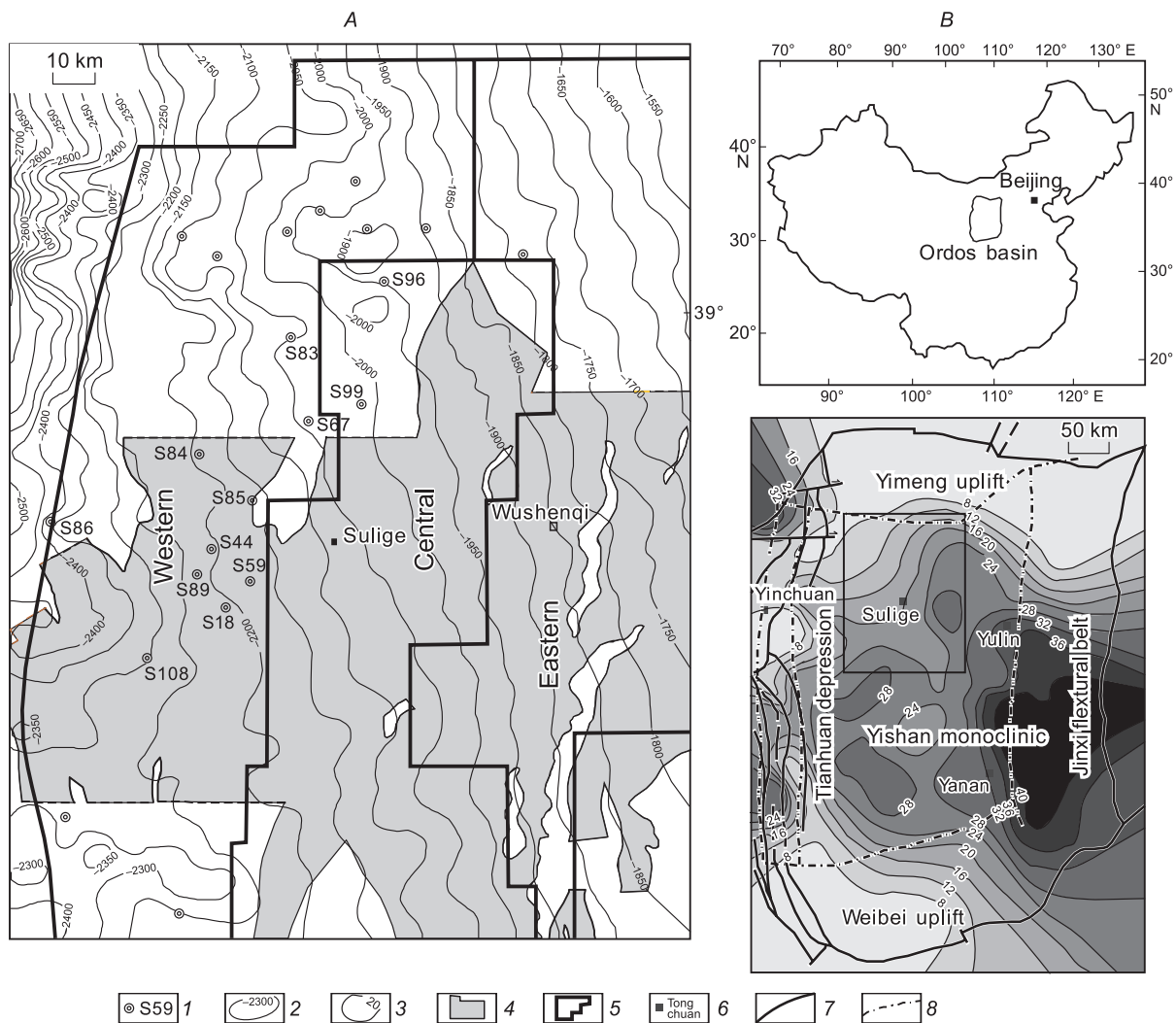
Fig. 1. The location of study area in Ordos basin and regional structure. (*A*) Structure contour map on the bottom of He 8 Member. (*B*) Regional location map of Ordos Basin and the hydrocarbon generating intensity map.

1, well name; *2*, bottom of H8; *3*, hydrocarbon generaling intensity (10^8 m³/km²); *4*, proved reserve; *5*, sulige gas field; *6*, town; *7*, fault; *8*, structural units boundary.

hydrocarbon-generating intensity in the east (>20×10^8 m³/km²). The He 8 gas reservoirs have the typical characteristics of less efficient gas charging due to insufficient source rocks. In terms of the entire Sulige region, due to different hydrocarbon-generating intensity, the He 8 gas reservoirs produce water ubiquitously in the west and produce little water in the east (Dou et al., 2010). Taking the Su-59 well area in the west of Sulige as an example, a total of 74 wells have been drilled in this area. In the He 8 member, the numbers of gas wells, water-bearing gas wells and water wells represent 7%, 24% and 69% of the total number of wells, respectively. Producing water in gas wells has become the bottleneck restricting the exploitation and development of this type of gas reservoirs. The key to using this type of reserve is to search the gas-rich regions and to avoid the high water producing regions.

1 GEOLOGICAL BACKGROUND

The Ordos Basin is located in north central China. It is the second largest sedimentary basin in China, with an area of 37×10^4 km². Tectonically, this basin belongs to the western portion of North China platform, and is a large polycyclic sedimentary basin with stable settlement and depression migration. The main body of the basin is the Yishan Slope, and the internal fracture is undeveloped. The formation shows a gentle monoclinic structure that is west-dipping, with a dip angle of less than 1° (Figure 1). The basin is very rich in oil and
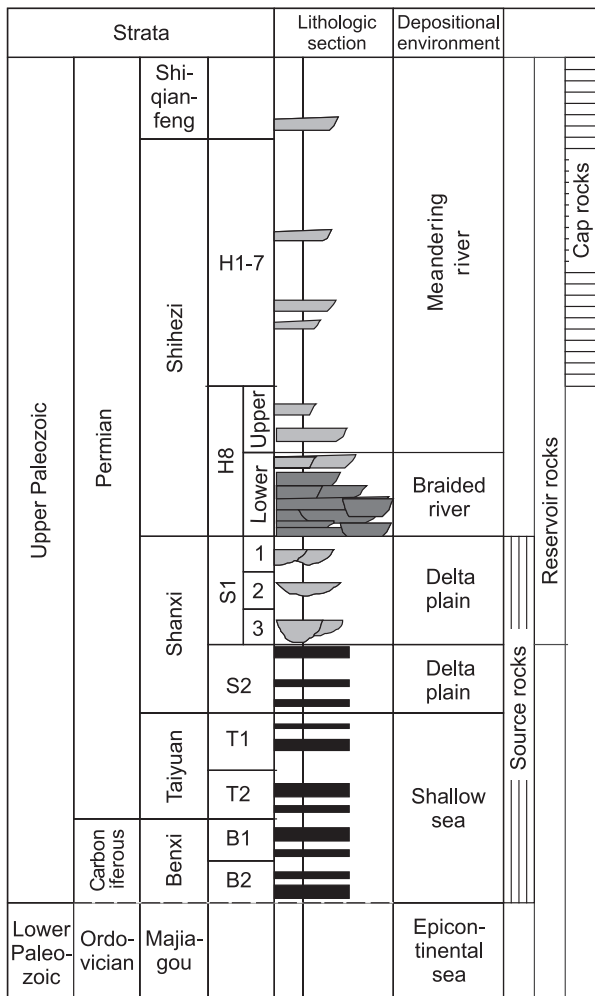
Strata			Lithologic section	Depositional environment		
Upper Paleozoic	Permian	Shi-qian-feng		Meandering river		Cap rocks
		Shihezi / H1-7				
		H8 Upper			Reservoir rocks	
		H8 Lower		Braided river		
		Shanxi S1 1		Delta plain		
		Shanxi S1 2		Delta plain		
		Shanxi S1 3				
		S2		Delta plain	Source rocks	
		Taiyuan T1				
		Taiyuan T2		Shallow sea		
	Carboniferous	Benxi B1				
		Benxi B2				
Lower Paleozoic	Ordovician	Majia-gou		Epicontinental sea		

Fig. 2. Stratigraphic distribution of main source rocks, reservoir rocks and cap rocks, and depositional environments in Upper Paleozoic of west Sulige, Ordos Basin.

gas resources. The southern basin mainly produces oil, whereas the northern basin produces mainly gas. The oil originates primarily from the Mesozoic Triassic and Jurassic, and the natural gas originates mainly from the Paleozoic.

The Caledonian movement in the Ordovician period uplifted the Ordos platform over a large area. This initiated the seawater retreat in westerly and southerly directions, rendering the entire region a denuded zone. Therefore, the Late Ordovician – Early Carboniferous deposits are missing in the Ordos platform (Figure 2) (He et al., 2003). In the late Carboniferous, seawater invaded from the east and west, forming the Carboniferous Benxi – Permian Taiyuan Formation coal-bearing clastic-carbonate rocks. After evolvement of the Taiyuan Formation, the seawater began to withdraw, forming the transitional facies coal-bearing deposits. Subsequently, the paleoclimate changed from warm and humid to hot and dry and tectonic uplifting occurred in Inner Mongolia in the north of the basin. The sediment supply was ample, and the lake range further shrunk toward the south.

At the bottom of the Shihezi Formation in the northern basin, thick coarse-grained braided sandstones got developed. Subsequently, because of the weakening of the uplift, the sediment supply was reduced, and the sedimentary facies turned from braided-stream into meandering-stream (Xie et al., 2013).

From the bottom to the top, the Upper Paleozoic is composed of the Carboniferous Benxi Formation, the Permian Taiyuan Formation, Shanxi Formations, Shihezi Formation and Shiqianfeng Formation. Depending on the lithology, the Shihezi Formation is divided into eight members, and the Shanxi Formation is divided into two members. He 8 and Shan 1 are the main gas-producing members. Source rocks are coal-bearing units deposited in Benxi Taiyuan and Shanxi Formation (Figure 2).

2 THE KEY ELEMENTS OF GAS RESERVOIR ACCUMULATION

2.1 Source rocks

In the Late Paleozoic, the Ordos Basin sedimented widespread paralic Carboniferous–Permian coal-bearing stratum above the Lower Paleozoic paleoerosion surface. The coalbed, carbonaceous shales and dark mudstones formed organic-rich source rocks, where the coalbed composed the main source rocks (Xiao et al., 2005). In the Upper Paleozoic of west Sulige, thickness of dark mudstones ranges between 25 and 35 m, and thickness of the coalbed is 4-8 m. But in the central and east Sulige, thickness of dark mudstones is 30-50 m, and thickness of the coalbed reaches 8-10 m. The abundance of source rocks in west Sulige is notably lower than that in central and east Sulige. The organic carbon content in the coalbed is 50-90%, with a total hydrocarbon concentration of 1.8-2.5%, a hydrocarbon production potential (S1 + S2) of 71.9-78.1 mg/g (Yang et al,. 2007). In the dark mudstones associated with the coalbed, the organic carbon content is 1.0-5.0%. The hydrocarbon generation mechanism is similar to that in the coalbed, and the hydrocarbon production potential of these mudstones is also rather high. The abundance of organic matter in the Upper Paleozoic source rocks is relatively high, and areas with hydrocarbon production intensity greater than 10×10^8 m^3/km^3 account for more than 71.6% of the total area of the basin. The total hydrocarbon production is 563.11×10^{12} m^3 (Yang et al., 2007).

In the previous studies thermal evolution of the Basin was divided into four stages (Gao and Ren, 2006). 1) The first stage lasted from the sedimentation of Upper Paleozoic source rocks to the end of Triassic. During

this stage, the basin did not experience major tectonic activity, and the burial depth steadily increased. Most of the organic matter did not enter the mature period, and the formation was basically under a normal range of pressure. 2) The second stage lasted from late Triassic to end of the Middle Jurassic. Due to a further increase in the burial depth, organic matter generally entered the mature stage. The constantly generated natural gas displaced the pore water. Due to dense lithology, the overall pressure increased, and abnormally high pressure was registered locally. 3) The third stage lasted from Late Jurassic to the Early Cretaceous. The maximum paleo-burial depth was reached. In addition, under the influence of Yanshan tectonic thermal events (Zhao and Behr, 1996), the organic matter entered the dry gas generation stage. This was the main stage of gas formation in Sulige. The gas supply in the reservoir was much larger than the gas loss, and the formation pressure generally increased, causing the extensive high-pressure state of the gas reservoirs. This was the main factor of abnormally pressured gas reservoir (Meckel and Thomasson, 2008; Spencer, 1987). 4) The fourth stage began after the early Cretaceous. The formation was uplifted and temperature decreased. The gas that was absorbed in the source rocks was resolved, becoming a new source supply of gas. However, the amount of these gas sources was limited, and the hydrocarbon generation gradually decreased, and eventually stopped (Jia et al., 2005). The temperature decreased in the gas reservoir and the late loss of gas led to a reduction in the pressure of the gas reservoir. Abnormally high pressure was no longer the case, and the gas reservoir pressure gradually changed from high to low.

2.2 Reservoir quality

The lower part of the He 8 Member consists mainly of braided-stream facies. The single channel sandstone thickness is 0.2-1 m. However, because of the rapid streams of the braided river, the fluvial channel is wide and shallow, and the lateral migration is fast. Braided-stream channel sandstones cut each other in the longitudinal directions, and expose amalgamated complexes, the total thickness of which reaches up to 30 m (Figure 3). The upper part of the He 8 member is represented by meandering-stream facies. The sandstones are less developed than the lower part, exhibiting "mud wrapping sand" characteristics along the profile. The single channel sandstone thickness is 0.2-2 m, and the total thickness 20 m.

The He 8 Member consists mainly of fine- to coarse-grained sandstones and mudstone. Coarse-grained sandstones contain gravel to varying degrees, and shares of sublitharenite and litharenite are 30% and 70%, respectively. In middle-grained sandstones, the proportions of sublitharenite and litharenite are 13% and 87%, respectively. Fine sandstones are composed entirely of litharenite. Rock fragments contain mainly quartzite, phyllite, schist, argillite, mica and volcanic rocks, but feldspar is almost abscent.

Coarse-grained sandstones develop mainly in the middle and lower portions of the fluvial channels (Figure 3). Some fluvial channels are completely composed of coarse-grained sandstones. In general, the quartz content is high and the rock fragment content is low in coarse-grained sandstones. Due to strong quartz overgrowth, the intergranular pores are poor. The acidic water in the coal-bearing strata causes unstable minerals, such as epimetamorphic rocks and volcanic rocks, to dissolve. Intergranular dissolved pores, moldic pores and intergranular micropores are developed. The throat is a flat space formed after quartz overgrowth, where a small amount of clay filling can be seen (Figure 4 *A, B*). The stress sensitivity of coarse-grained sublitharenite is relatively weak. Under 40 MPa overburden pressure, the permeability is approximately 40% of the ground permeability, showing an overburden pressure permeability of 0.1-0.3 md. The stress sensitivity of coarse-grained litharenite is relatively strong. Under 40 MPa overburden pressure, permeability decreases to approximately 4% of the ground permeability, showing an overburden pressure permeability of 0.0007-0.006 md (Figure 5).

Medium-grained sandstones develop mainly in the middle and upper parts of the fluvial channels. The rock fragments content is substantially higher compared to coarse-grained sandstones. Strong compaction causes most of the ductile rock fragments to deform and weakens quartz overgrowth in sandstones. Although rock fragments dissolution occurs, the dissolution products are not fully brought out, and the pores are primarily intergranular dissolved pores and intergranular micropores. The throat is often filled with various types of clay minerals and exhibits a bundle or honeycomb shape (Figure 4 *C, D*). Medium-grained sublitharenite is characterized by weak stress sensitivity. Under 40 MPa overburden pressure, the permeability is approximately 31% that of the ground permeability and the underground permeability is 0.02-0.06 md. The stress sensitivity of medium-grained litharenite is very strong. Under 40 MPa overburden pressure, the permeability drops to approximately 2.7% that of the ground permeability and the overburden pressure permeability is 0.001-0.003 md (Figure 5).

The porosity of fine- to medium-grained sandstones does not change much in the presence of the overburden pressure, which suggests that the volume of the throat occupies a small proportion of the total pore volume, and reflects a strong cementation effect.

The fine-grained sandstones are all litharenite, with a rock fragments content of approximately 47%, which is the highest among sandstones of all grain sizes. A large amount of epimetamorphic rock fragments and
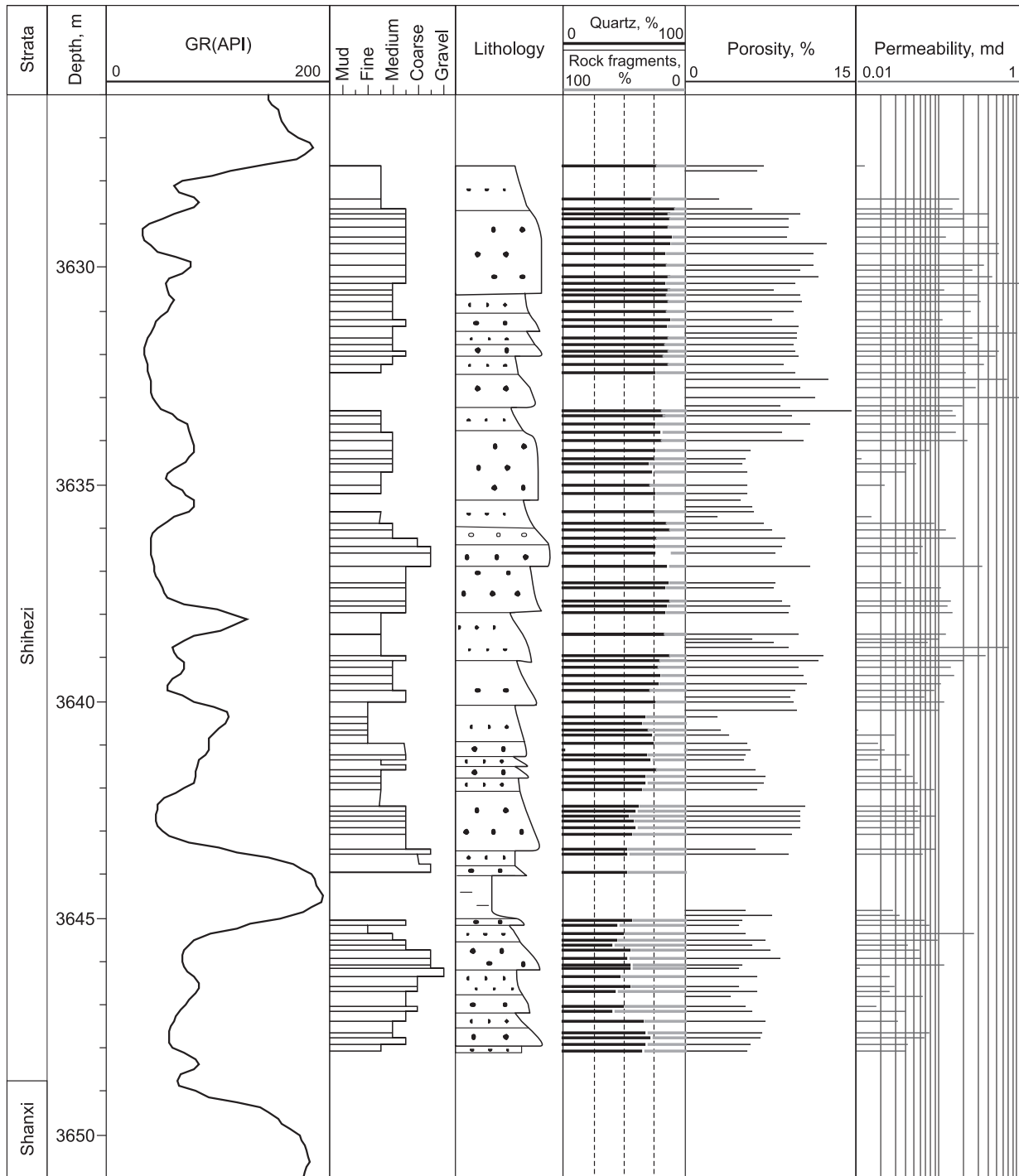
Fig. 3. Lithologic and petrophysical section of He 8 interval of Well Su59-4-13. There is a good correlation between quartz content and reservoir quality.

volcanic rock fragments causes strong compaction, and detrital fragments demonstrate long contact or concavo-convex contact, with almost no quartz overgrowth (Figure 4 *E*, *F*). The pores are primarily micropores formed from alteration of rock fragments. Occasionally isolated dissolved pores, formed by dissolution of rock fragments, can be observed. The throats are basically filled with pseudomatrix and thus not continuous, resulting in some isolated pores. The stress sensitivity of this type of reservoirs is similar to or stronger than that of medium-grained litharenite.

Through the above analysis, it is evident that particle size is associated with rock fragments content to a certain extent. The larger the particle size, the lower the rock fragments content. For epimetamorphic rocks
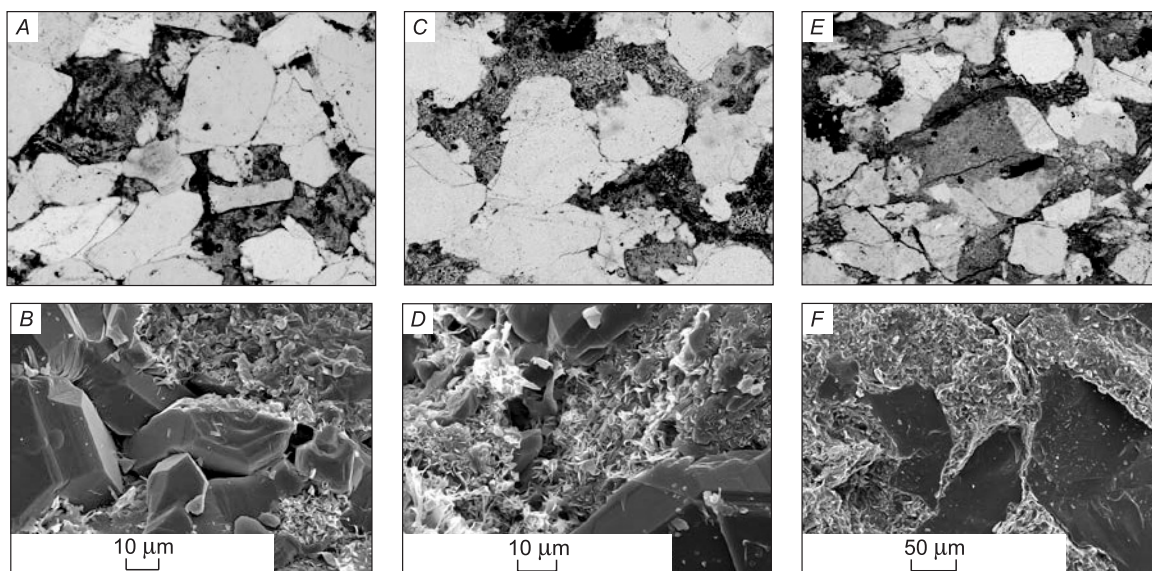
1356

Fig. 4. Thin-section photomicrographs of tight-gas sandstones and scanning electron microscope photographs. *A*: Intragranular dissolved pores are common and the throat is the flat space after quartz overgrowth; coarse-grained sublitharenite, well S59-4-13, 3629.9 m, X40, PPL. *B*: There is a relatively small amount of clay in the throat, which shows a triangular shape; coarse-grained sublitharenite, well S59-13-51B, 3537.4 m; *C*: Intergranular pores and micropores are common; medium-grained sublitharenite, well S594-13, 3629.2 m, X40, PPL; *D*: The throat is filled with clay, and shows a honeycomb shape; middle-grained sublitharenite, well S59-13-51B, 3526.2 m; *E*: The pores are all micropores, with a relatively small number of visible pores; fine-grained litharenite, well S59-4-13, 3919.5 m, X40, PPL; *F*: The throat is obstructed by ductile rock fragments; fine-grained litharenite, well S59-13-51B, 3519.3 m.

mainly consisting of phyllites, schists, shales and other rocks, rupture may easily occur along cleavage and lineation, forming fine-grained fragments, which will be deposited in regions with weak hydrodynamics. In regions with strong hydrodynamics, the main deposits are quartz grains (Nan et al., 2005). Under strong compaction effect, ductile grains show ductile deformation, reducing intergranular volume while weakening dissolution. This deteriorates the reservoir quality and complicates the pore structure. Under overburden pressure, ductile grains may also easily deform to close the throat, leading to increased stress sensitivity. Therefore, for the fine- to coarse-grained thick amalgamated sandstones the heterogeneity is considerable (Figure 3).

2.3 Traps and cap rocks

The focus of studies on conventional reservoirs is traps and it is thought that unconventional gas is often not controlled by traps. However, recent studies analyzed by Shanley et al. (2004) and Law and Curtis (2002) have shown that gas accumulation in many tight sandstones is still controlled by traps, such as the Jonah tight gas and the Hay tight gas in the Green River Basin (Shanley et al., 2004).

The west Sulige is located on the west side of the Yishan Slope, immediately adjacent to the Tianhuan
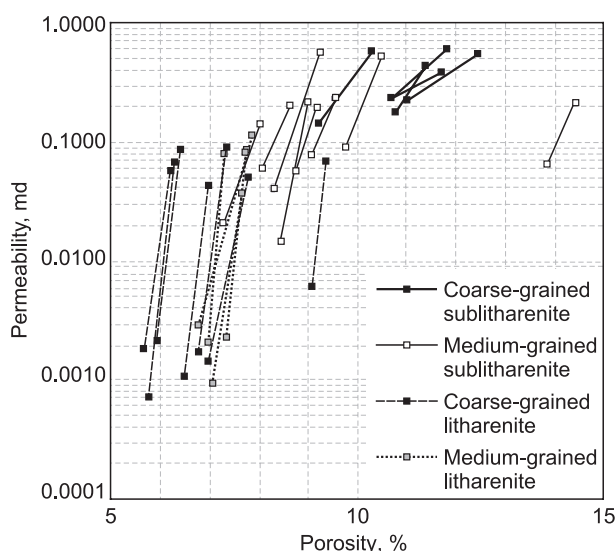

Fig. 5. Plot of porosity and permeability of different grain sizes and components at varying levels of net overburden stress illustrating the effect of overburden stress on porosity and permeability. For each core sample, two levels of net overburden are shown: ambient condition 0 MPa and 40 MPa.

syncline (Figure 1). Strong tectonic movements have made the local structural trap of this region more developed than the eastern part of the Yishan Slope. Under the monoclinic tectonic background of this region, a series of low-amplitude structural traps have developed. The He 8 thick sandstones are separated by a series of mudstones between fluvial channels extending along the north-south direction, forming a number of updip pinch-out lithologic traps. As can be seen in Figure 6, for He 8 sandstones in well S59-11-42 on the west side of the overbank mudstones, because it is located at the updip pinch-out, the natural gas is relatively enriched. This well has initial production rate 8.64×10^4 m^3 gas/d, and does not produce water. The well S298 at its base produces water without gas. In contrast, the He 8 sandstones in well S59-12-50 on the east side of the overbank mudstones are located at the bottom of the structure, and the initial production rate is 2.46×10^4 m^3 gas/d. The water production rate is 5.0 m^3/d, and hence this region is relatively water enriched. The position of well S59-13-54 is higher than that of S59-13-51. However, the initial production rate in well S59-13-54 is 2.17×10^4 m^3 gas/d, with a water production rate of 10.0 m^3/d, whereas the initial production rate in the lower positioned well S59-13-51 is 7.29×10^4 m^3 gas/d. This may be because the reservoir quality of well S59-13-54 in higher structure is tight, and gas displacement is poor.

The He 8 gas reservoir was formed in the Early Cretaceous. After gas accumulated, intense tectonic uplift occurred, and the uplift amplitude was close to 1000 m. The cap rocks play an important role in gas preservation. The regional cap rocks in the He 8 tight-gas are the thick mudstones in the Shihezi and Shiqianfeng Formations, and the direct cap rocks are the mudstones and tight stratum in the He 7, He 6 and He 5 Members. Thickness of the direct cap rocks is 80-120 m. The cap rocks are formed via thinning of the throat and reduction in gas and water permeability. However, gas and water can still be transported slowly. Thus, for the cap rocks, the seal is relative, whereas loss is eternal. When hydrocarbon generation is greater than hydrocarbon loss, gas accumulation in the tight sandstone reservoirs occures; otherwise, natural gas dissipation occurs.

2.4 Migration and loss of natural gas

In the Late Jurassic –the Early Cretaceous, tectonic thermal events resulted in an increase in the palaeogeothermal gradient of the basin of 3.1-4.5 °C/100 m (Ren, 1995; Zhao and Behr, 1996). Thermal events lasted 80 Ma, and the coal-bearing strata began to produce large amounts of gas. Based on the methane content in gas, the drying coefficient, density, carbon isotope and other evidence (Cao et al., 2011), it is believed that the dis-
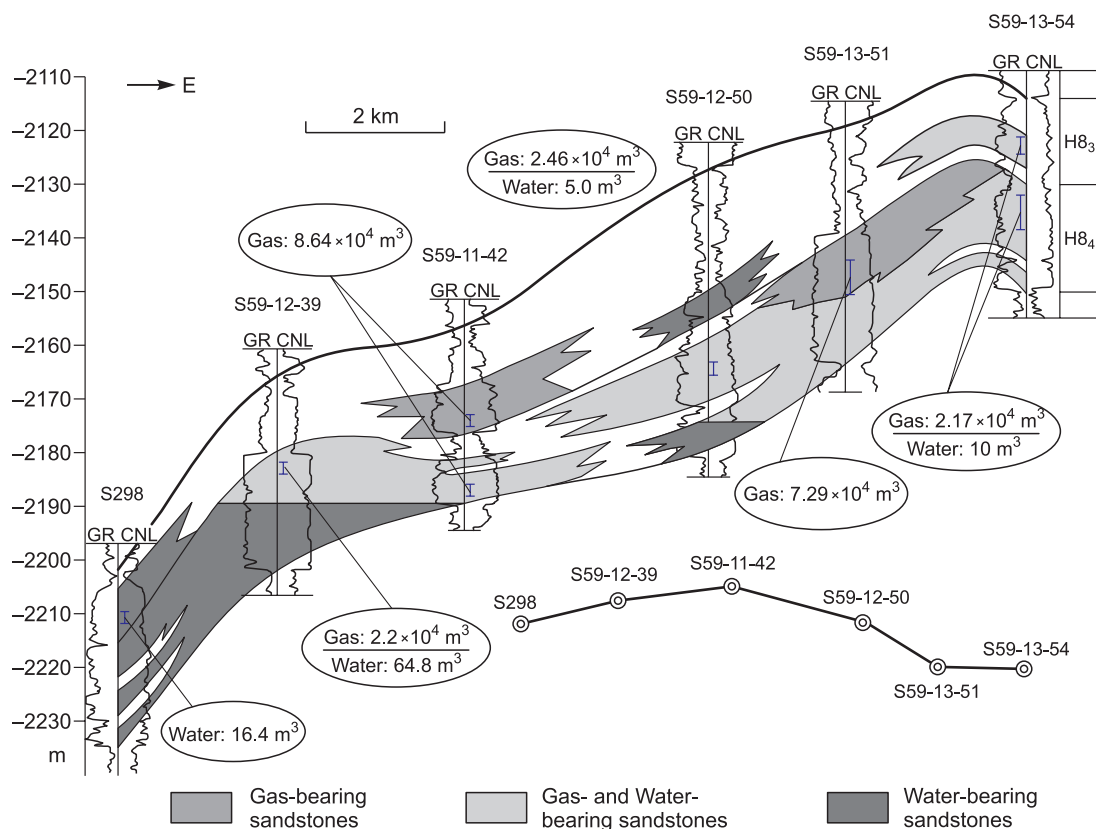

Fig. 6. Cross section of He 8 interval illustrating gas and water distribution.

tribution of gas is a result of near-source short distance migration and accumulation, and there has been no long-distance lateral migration of natural gas. The gas generated by underlying source rocks migrates upward and charges the reservoirs above, resulting in a gradually decreased charging efficient from bottom to top. The number of gas wells with no water production in the Shan 1 Member is substantially higher than that in the He 8 Member.

After the Early Cretaceous, the Yanshan orogeny uplifted the overall basin. The temperature decreased, and gas generation nearly stopped. Basin modeling suggests that the gas generation intensity in the Upper Paleozoic coal-bearing source rocks was 2.84×10^8 m³/km² in the Middle Jurassic (Liu et al., 2000); it increased to 18.57×10^8 m³/km² in the Early Cretaceous, and decreased to 1.25×10^8 m³/km² in Late Cretaceous. Hence, after the formation of the Upper Paleozoic tight-gas reservoirs, there was a lengthy process of gas loss. Based on the diffusion coefficient of the cap rocks, it is estimated that the amount of natural gas diffusion is 1.28×10^8 m³/km², i.e., 2.6 fold that of the total accumulation amount (accumulation coefficient 4%).

The gas reservoir pressure depends on the amount of natural gas loss as well as the amount of gas generation by the source rocks (Meissner, 2000). Wushenqi and Yulin are located in a high hydrocarbon generation area, where the gas reservoir pressure is high. Gas reservoirs in this area are mostly with no water production, suggesting that the amount of gas generation by source rocks can compensate for the loss of natural gas to some extent and slow down the reduction in the gas reservoir pressure (Xu et al., 2011).

3 DISCUSSION

3.1 Sandstone densification and gas charging

The densification of sandstones in the He 8 Member was completed primarily in two forms: strong compaction densification of litharenite and compaction – silica cementation densification of sublitharenite. Tight sandstones formed by strong compaction have low silica cement content, and ductile grains deformation makes the detrital particles exhibit long, concavo-convex contact. From the perspective of low cement content and the burial history (Figure 7), densification of litharenite occurred early, and was completed before gas charging. For tight sublitharenite formed by compaction – silica cementation, the compaction caused a 24.4% loss of porosity. Subsequently, due to gas charging and increase in gas reservoir pressure, compaction weakened. Then, silica cement further deteriorated the reservoir quality. Fluid-inclusion data show that the inclusion types in the quartz overgrowth side include gaseous hydrocarbon inclusion, liquid hydrocarbon inclusion and brine inclusion. The homogenization temperatures lie mainly in the range from 90-120 °C up to 140 °C. In other words, natural gas charging occurred at the same time as quartz overgrowth or slightly later, which is characteristic of simultaneous densification and gas accumulation. Therefore, for sublitharenite, the porosity before gas charging should be approximately 3-4% higher than the current porosity. The heterogeneity of reservoirs at the time of gas charging was greater than the current heterogeneity of the reservoirs, and the porosity of the sublitharenite was relatively high.

In this condition, natural gas charged sublitharenite because of the strong permeability difference, of which the physical properties were suitable for gas charging. For the tight sandstones formed by strong compaction, efficient charging of gas was poor due to high displacement pressure. Thus, the different processes of sandstone densification led to differences in the displacement pressure of the reservoirs during gas charging, eventually resulting in differences in gas saturation.

3.2 The impact of regional structure on natural gas accumulation

The top surface of the tight-gas reservoirs in west Sulige depends on the structure and the thickness of the sandstones. If the regional structure is monoclinic, the sandstone-rich region can form a regional structure caused by differential compaction. The sandstone thickness in the He 8 Member is 20-30 m, and is composed of several braided-stream fluvial channel sandstones. Because the sandstones extend along the north-south direction, whereas the regional structure shows a monoclinic westward, the continuity of the fluvial channel sandstones in the west-east direction is relatively poor. The height of the He 8 regional structures can reach 40-50 m. Considering that the sandstone thickness is 20-30 m, we deduce that the height of the continuous gas column can reach 70 m, producing a buoyancy of approximately 0.7 MPa.

To examine the effect of 0.7 MPa buoyancy on gas charging, six sublitharenite samples were tested in order to determine the capillary pressures and relative permeability (Figure 8). First, P_{Hg}, which was obtained from mercury capillary pressure, was converted into gas/water capillary pressure P_{wg}, using the following formula:

$$P_{wg} = \frac{\sigma_{wg} \cos \theta_{wg}}{\sigma_{Hg} \cos \theta_{Hg}} P_{Hg} = \frac{72 \times \cos 0°}{480 \times \cos 140°} P_{Hg} \approx \frac{1}{5} P_{Hg}$$

System period	C	P	T_{1-2}	T_3	J_1	J_2	J_3	K_1	K_2	E-Q

Time, Ma: 280 — 200 — 120 — 40

Burial history curve

Late Indosinian movement
Early Yanshanian movement
Middle Yanshanian movement
Late Yanshanian movement

(depth axis: 1, 2, 3, 4 km)

Ro, % — 0.5   0.7   1.3   1.75

Paleogeotemperature, °C — 65   99   136   150

Gas generation stages — no gas generation | begin to generate | intense generation | stop generating

Evolution of pressure — (axis: 1.4, 1.2, 1.0, 0.8)

Diagenetic sequence — Early diagenesis | Late diagenesis: A_1 | A_2 | B_1 | B_2

Pore evolution of sublitharenite, %
38 — compaction −24.4 → 13.6 — dissolution +1.8 / overgrowth of quartz −7.2 → 8.2 — dissolution +1.8 / precipitation −2.1 → 7.9 — microfracture +0.5 → 8.4

Pore evolution of litharenite, %
38 — compaction −30.2 → 7.8 — dissolution +0.7 / overgrowth of quartz −2.3 → 6.2 — dissolution +0.2 / precipitation −2.4 → 3.9 — microfracture +0.5 → 4.4
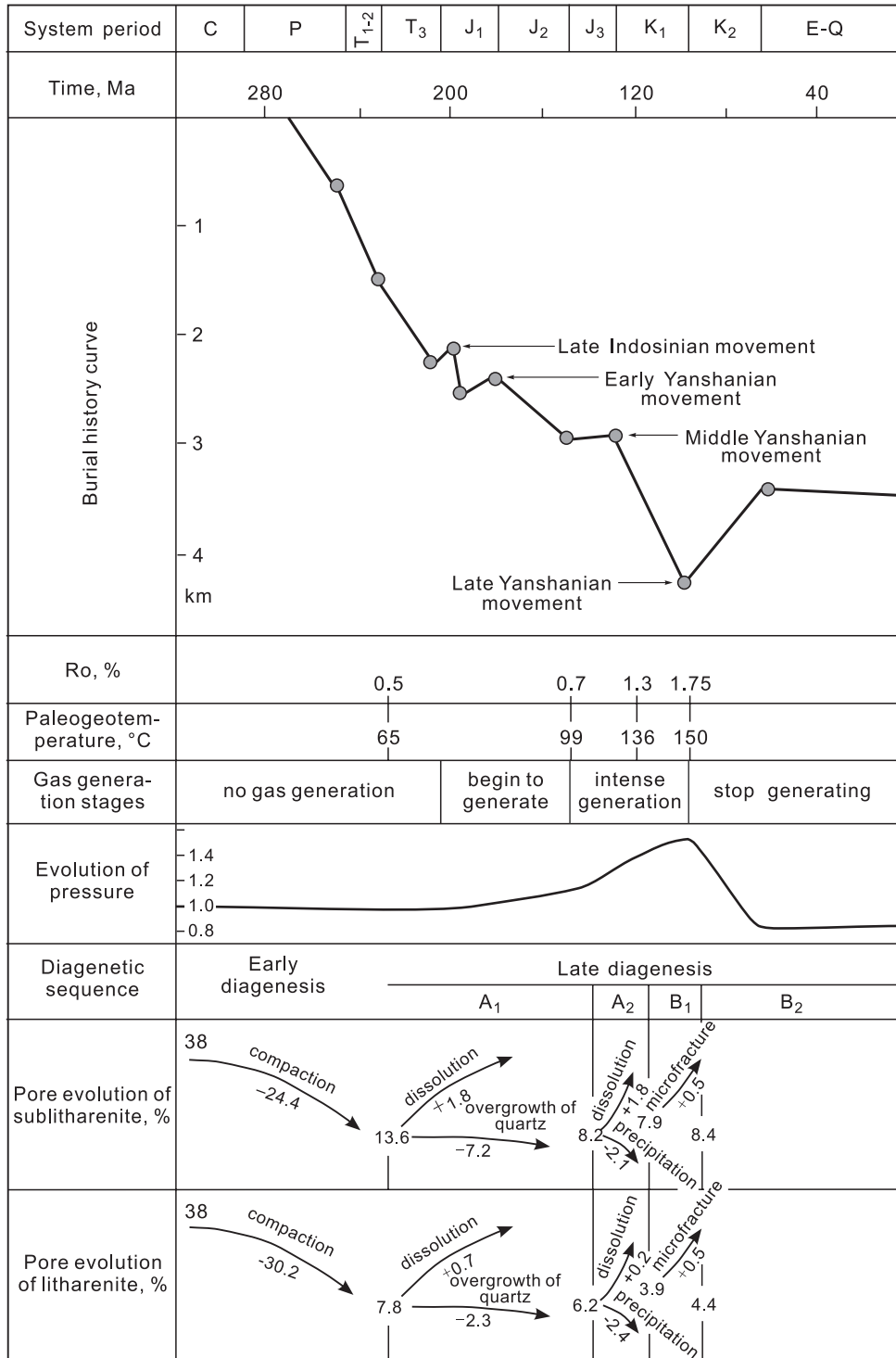
Fig. 7. The burial history, hydrocarbon generation history and reservoir porosity evolution of the He 8 Member. During peak of gas generation, porosity of sublitharenite is markedly better than that of litharenite.

P_{wg}: gas/water capillary pressure, MPa; P_{Hg}: mercury capillary pressure, MPa; σ_{wg}: gas/water interfacial tension, mN/m, here the value is 72 mN/m; σ_{Hg}: mercury/water interfacial tension, mN/m, here the value is 480 mN/m; θ_{wg}: gas/water wetting angle, here the value is 0°; θ_{Hg}: mercury/water wetting angle, here the value is 140°.
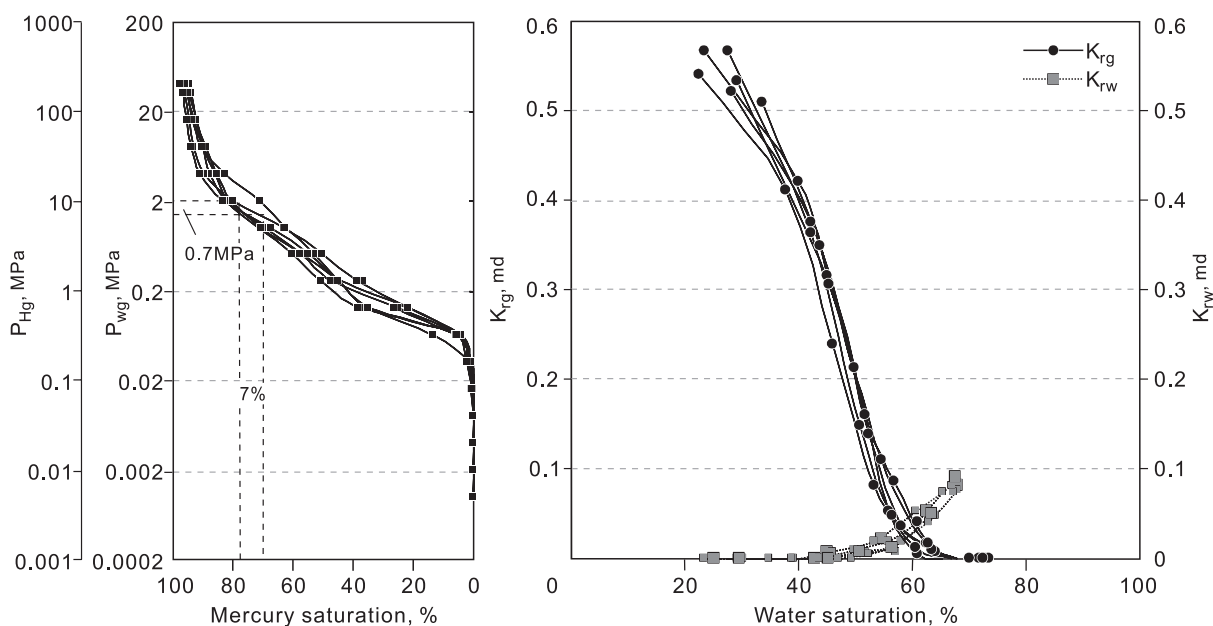
Fig. 8. Relative permeability and capillary pressure curves of coarse-grained sandstones.

The average gas saturation of the six coarse-grained sandstones samples is 71%, and the corresponding gas/water capillary pressure is 1.3 MPa. If a 0.7 MPa pressure is imposed, the gas saturation is increased by 4-10%, with a mean of 7% (Figure 8). From the above analysis, we know that when natural gas began charging, the quality of the coarse-grained sandstones was slightly better than that of the current reservoirs. Thus, at that time, the increase in gas saturation caused by the regional structure likely exceeded 7%. It can be seen that buoyancy caused by regional structures can increase the gas saturation in reservoirs with good physical properties, but such increases in reservoirs with poor physical properties are not obvious.

3.3 The impact of tight sandstone heterogeneity on gas accumulation

After the Permian Shanxi Formation sedimentation, the short tectonic uplift elevated the base level, and the shoreline apparently shifted towards the lake, reducing the accommodation space. At this point, the braided stream was wide and shallow. Due to frequent migrations and erosions, a large number of coarse-grained clastic materials were deposited. Braided stream fluvial channels sandstones were amalgamated, showing a blanket-like distribution along the horizontal directions. According to lithology statistics of eight coring wells, coarse-, medium- and fine-grained sandstones account for 65%, 16%, and 19%, respectively. The single fluvial channel sandstones show fining upward succession. The larger the grain size, the lower the content of ductile grains, which indicates coarse-grained sandstones have better reservoir quality because of weak ductile clastics deformation (Figure 3). The lower displacement pressure reduces the resistance to gas charging and is conducive to gas accumulation.

Previous studies have shown that when the pore-throat sizes of tight sandstones are less than 2 μm, buoyancy is not the dominant force in forming and maintaining the distribution of gas in tight-gas accumulation. Thus, pore-throat sizes of 2 μm are considered to be the boundary between conventional gas and tight-gas. From capillary pressure curves (Figure 9) it can be seen that for sublitharenite, pore-throat sizes greater than 2 μm account for 48.2% of the total pore volume, and buoyancy is still the dominant force of gas accumulation. For litharenite, however, gas accumulation via the buoyancy rarely occurs because pore-throat sizes greater than 2 μm accounts for 13.5% of the total pore volume.

Although the lateral continuity of the braided-stream fluvial channel sandstones is good, different reservoir physical properties result in differences in gas charging, causing frequent isolation and scattering of gas-bearing sand bodies, which are separated by tight sandstones with high water saturation. For example, in well S59-5-13B (Figure 10), the interval located at 3848.9-3542.3 m belongs to coarse-grained sublitharenite, showing good physical properties. This interval is basically free of micropores, and the pores are primarily free fluid pores; differential spectra and total hydrocarbon data suggest it is a gas-bearing layer. The 3542.3-3538.0 m interval is composed mainly of coarse litharenite; the porosity does not vary much, but the permeability is sub-
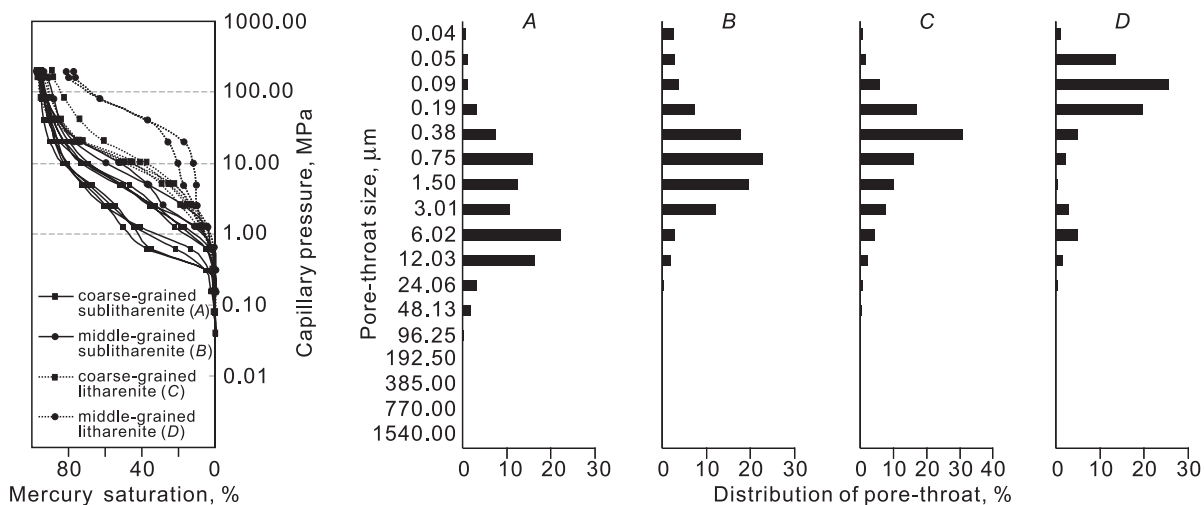
1361

Fig. 9. The capillary pressure curves and pore throat size distributions of different types of reservoir beds. *A*: Pore-throat distribution of coarse-grained sublitharenite; *B*: Pore-throat distribution of middle-grained sublitharenite; *C*: Pore-throat distribution of coarse-grained litharenite; *D*: Pore-throat distribution of middle-grained litharenite.

stantially reduced compared with the previous interval. In addition, there is a large number of micropores in the reservoir space and free fluid porosity is reduced. Differential spectra and total hydrocarbon data both detect abnormality, but the abnormality is not obvious, and the result can be interpreted as a gas-water layer. The 3538.0-3530.8 m interval contains primarily medium- to coarse-grained litharenite, with local fine-grained litharenite. The permeability is one order of magnitude lower than the sandstones in 3848.9-3542.3 m; the free fluid porosity is substantially reduced, replaced by a large amount of micropores, and differential spectra and total hydrocarbon data both suggest that it is the water-bearing layer. The 3542.3-3527.3 m interval contains medium-grained sublitharenite, which shows good physical properties. Here, free fluid pores and micropores coexist; the differential spectra detects abnormality, but as the thickness is small, total hydrocarbon data does not reveal noticeable abnormality, and the result is interpreted as the gas–water layer. The 3527.3-3525.0 m interval consists of fine- to medium-grained litharenite, showing poor physical properties; the reservoir space is composed of a large amount of micropores and both differential spectra and total hydrocarbon data suggest that it is a water-bearing layer. Finally, gas testing was performed on the 3548.9-3540.2 m interval. After fracturing, the gas production was 2.58×10^4 m³/d and water production was 12 m³/d.

Thus, it can be seen that for sublitharenite with relatively good physical properties, the intensity of gas charging is high, and the gas saturation is high. For litharenite, due to the presence of a large number of micropores, the gas displacement effect is poor, and water disperses in the gas reservoirs. In braided-stream fluvial channel sandstones, the strong heterogeneity leads to amalgamation of the gas-bearing layer, the gas–water layer and water-bearing layer. Such strong heterogeneity determines the difficulty of gas development. Water-bearing layers that are sandwiched in tight-gas sandstone reservoirs are also rather common in other basins in the world.

3.4 The impact of tectonic uplift on natural gas accumulation

The Cretaceous Yanshan tectonic movement caused the overall Ordos platform to be uplifted nearing 1000 m. The tight-gas reservoirs pressure dropped by 24.9-25.6 MPa, or 47-49%, and the temperature decreased by approximately 60 °C, or about 36%. Because the Upper Shihezi Formation in different parts of Sulige shows gas, the gas is considered to be caused by natural gas loss. By comparing the pressure loss due to the decrease in the formation temperature and the actual amount of pressure loss, it can be found that the pressure loss caused by the temperature decrease accounts for 73-77% of the total pressure loss, whereas the pressure loss due to the loss of natural gas accounts for 23-27% of the total pressure loss.

The temperature drop and gas loss can result in a decline of the reservoir pressure (Law, 2002). However, for tight sandstones with no natural gas charging or mudstones near the tight-gas reservoirs, there is no gas loss, and the pressure will not decrease substantially even with a temperature decrease. Thus, these tight sandstones or mudstones are of normal or slightly high pressure (Law and Dickinson, 1985). Hence, after the
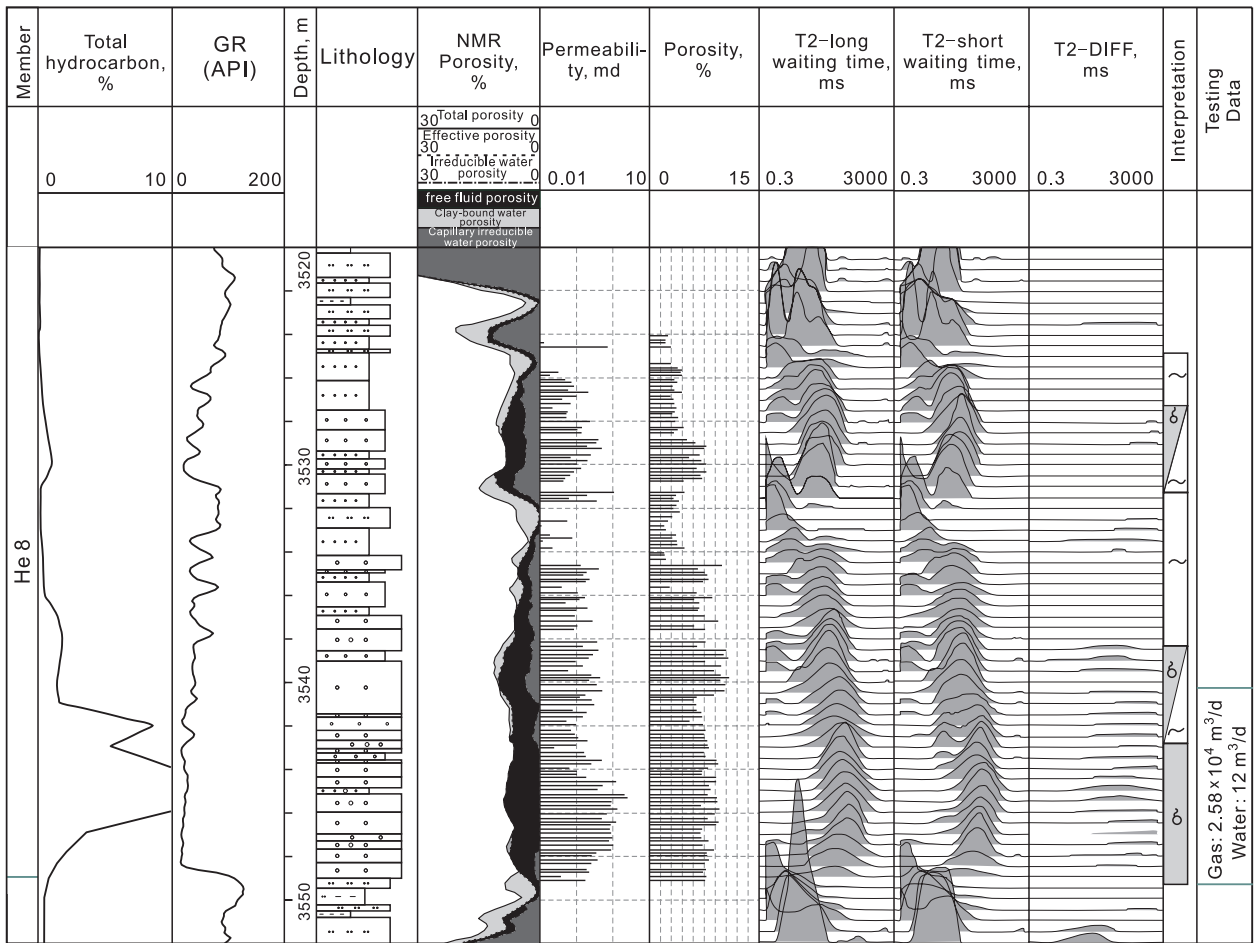
Fig. 10. The integrated physical property – well logging – gas testing chart of well Su 59-5-13B.

Yanshan tectonic movement at the end of the Early Cretaceous, there had pressure differences between the tight-gas reservoirs and the nearby water-bearing tight sandstones or mudstones. Water in the water-bearing tight sandstones and mudstones flew towards the low-pressure tight-gas sandstones to correct this pressure imbalance (Law, 2002; Law and Dickinson, 1985). After being "sucked" into the tight-gas reservoirs, water would migrate to a lower position under the effect of gravity if the physical properties of the tight-gas sandstones were good. If the physical properties of the tight-gas reservoirs were poor, water would be distributed in the throat, disperse, and separate the continuous gas in the pores. Because the He 8 sandstones comprise amalgamated fluvial channel sandstones, the particle size of sandstones is fine at the edge of the braided-stream fluvial channels, which show a high level of ductile grains and poor gas accumulation. In the tectonic uplift and water absorption processes, these tight water-bearing sandstones divided the uncompartmentalized He 8 gas field into a multireservoir gas field with several gas/water interfaces, further complicating the gas and water distributions.

Figure 11, *A* simulates the He 8 gas pool at the end of Early Cretaceous when source rocks reached the peak of hydrocarbon generation. Except in the fine litharenite at the edge of the fluvial channel sandstones, where there was no natural gas charging due to extremely tight lithology, other fluvial channel sandstones were all charged with natural gas. After the Late Cretaceous, water was sucked into the low-pressure tight-gas reservoirs form normal pressure water-bearing sandstones or mudstones due to Yanshan tectonic uplift. If sandstones were sublitharenite, gas–water differentiation would occur, e.g., the tight-gas reservoirs composed of sand bodies 1a, 1b and 1c. If sandstones were litharenite, the water sucked into the low-pressure tight-gas reservoirs would diffuse in the tight sandstones, showing no obvious gas–water differentiation, e.g., the gas reservoirs composed of sand bodies 3a, 3b, 3c and 3d; the direct consequence was that the original gas reservoir was divided into several gas reservoirs.

Therefore, it can be seen that after the Yanshan tectonic uplift, the temperature decrease and loss of natural gas caused reduction in pressure of the tight-gas reservoirs, which then sucked water from nearby mudstones and tight water-bearing sandstones, further complicating the gas–water relationship in the gas reservoirs.

Table 1. **The pressure coefficients and unimpeded gas flows of the three wells of the Sulige gas field**

Well location	Formation pressure (MPa)	Pressure coefficient	Convert gas–water interface (m)	Gas open flow capacity (m³/d)	Water yield (m³/d)	Sands thickness (m)
Su44	32.05	0.92	1042.13	73025	0.7	25.3
Su59	32.95	0.96	1156.35	87825	0	12.7
Su18	28.73	0.82	704.51	15005	15.6	29.2

Taking the wells S44, S59 and S18 in the study area (Table 1) as examples, their pressure coefficients and converted gas–water interfaces varied considerably, suggesting that these wells belong to different pressure systems, and thus do not belong to the same gas reservoir. Hence, the He 8 tight-gas reservoir in west Sulige is a multireservoir gas field.

4 THE CHARACTERISTICS OF NATURAL GAS ACCUMULATION IN LESS EFFICIENT CHARGING TIGHT - GAS RESERVOIRS

Less efficiently charging tight-gas is a quasi-continuous gas between a conventional gas and a continuous gas. Less efficiently charging tight-gas is similar to conventional gas because it is controlled by traps to certain degree, and there may be relative enrichment of natural gas at high locations of the structure, and in updip pinch-outs. But there is diffused free water because of the poor quality of reservoirs and less efficient gas charging, and gas reservoirs that contain water are rather common. In addition, there is no regional gas–water interface, and the gas field is composed of multiple small superimposed gas reservoirs. Compared with continuous gas, similarities are close to the source rocks, tight reservoirs, extensive gas shows, but differ in that gas enrichment is controlled by intensity of gas generation, traps, reservoir physical properties and late gas loss in less efficient charging gas reservoirs. Buoyancy in less efficient charging tight-gas reservoirs contributes to gas accumulation to a certain degree.

Currently, reserves in less efficient charging tight-gas reservoirs are concentrated mainly in certain subtle traps. Natural gas is primarily accumulated in sublitharenite in structural traps and updip pinch-out traps. These types of tight-gas are mostly gas reservoirs without water production. However, natural gas occurs in diagenetic traps in monoclinic zones, controlled by the lateral seal of low-permeability layers. Because the structure
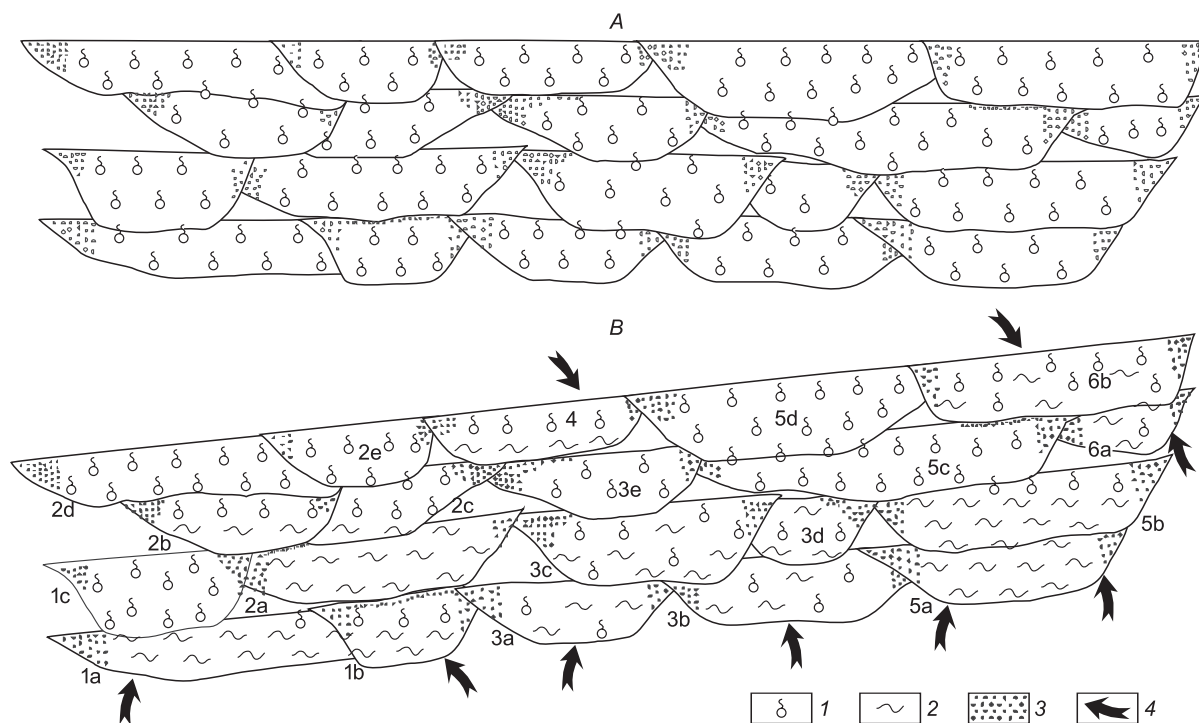

Fig. 11. Schematic model showing gas and water differentiation by tectonic uplift.

1, gas-bearing sandstones; *2*, water-bearing sandstones; *3*, super tight sandstones; *4*, water moving direction.

is relatively flat, gas–water differentiation is not complete. Gas reservoirs contain gas–water layers and water-bearing layers. This type of gas reservoir frequently produces gas and water at the same time, and gas production drops relatively rapidly.

5 CONCLUSIONS

1. Less efficient gas-charging is the main cause of the complex gas–water distribution in the He 8 gas reservoirs. The gas reservoir pressure drops due to the Yanshan tectonic uplift and the heterogeneity of the reservoirs aggravated the complication of the gas–water distribution, eventually causing the He 8 gas reservoir to become a multireservoir gas field with multiple gas–water interfaces.

2. The densification processes differ for two types of reservoirs, resulting in the fact that the heterogeneity of the sandstones at the time of gas-charging was stronger than that of current sandstones. Less efficient gas-charging causes the force for natural gas migration to be relatively low. The degree of gas-charging is high for sublitharenite because of the low displacement pressure. In contrast, due to the high displacement pressure in litharenite, gas-charging is difficult.

3. Sublitharenite is characterized by developed intergranular pores and intragranular dissolved pores. The majority of pores and pore throats are reduced to narrow slots. The reservoir physical properties are good with high overburden pressure. There may be edge and bottom water in the low parts of the trap, but no water production in the high parts. Litharenite is characterized by abundant micropores and bundle-shaped pore throats plugged by clay minerals and ductile grains. The reservoir physical properties are poor and natural gas displacement effect is low. Further, gas–water differentiation is very difficult, and a large amount of residual water is retained in the gas reservoirs.

REFERENCES CITED

Bates C.R., Phillips D.R., Grimm R. The seismic evaluation of a naturally fractured tight gas sand reservoir in the Wind River Basin, Wyoming // Pet. Geosci., 2001, v. 7(1), p. 35—44.

Camp W.K. Pore-throat sizes in sandstones, tight sandstones, and shales: Discussion // AAPG Bull., 2011, v. 95(8), p. 1443—1447.

Cao F., Zou C.N., Fu J.H., Yang Z. Evidence analysis of natural gas near-source migration-accumulation model in the Sulige large gas province, Ordos basin, China // Acta Petrol. Sin., 2011, v. 27(3), p. 857—866.

Cumella S.P., Shanley K.W., Camp W.K. Introduction // Understanding, Exploring, and Developing Tight-Gas Sands—2005 Vail Hedberg Conference. AAPG Hedberg Series, 2008, No. 3, p. 1–4.

Dai J.X., Ni Y.Y., Hu G.Y., Huang S.P., Liao F.R., Yu C., Gong D.Y., Wu W. Stable carbon and hydrogen isotopes of gases from the large tight field in China // Sci. China: Earth Sci., 2014, v. 57(1), p. 88—103.

Dou W.T., Liu X.S., Wang T. The origin of formation water and the regularity of gas and water distribution for the Sulige gas field, Ordos Basin // Acta Petrol. Sinica, 2010, v. 31(5), p. 767—773.

Gao S.L., Ren Z.L. Restoration of eroded thickness and its influence on thermal evolution of Upper Paleozoic source rocks in Ordos basin // Oil Gas Geol., 2006, v. 27(2), p. 180—186.

He Z.X. Evolution and hydrocarbon resources of the Ordos Basin. Beijing, Petroleum Industry Press, 2003, 390 p.

He Z.X., Fu J.H., Xi S.L. Geological features of reservoir formation of Sulige gas field // Acta Petrol. Sin., 2003, v. 24(2), p. 6—12.

Hirst J.P.P., Davis N., Palmer A.F. The tight gas challenge: appraisal results from the Devonian of Algeria // Petrol. Geosci., 2001, v. 7(1), p. 13—21.

Hood K.C., Yurewicz D.A. Assessing the Mesaverde basin-centered gas play, Piceance Basin, Colorado // Understanding, exploring, and developing tight-gas sands / Eds. S.P. Cumella, K.W. Shanley, W.K. Camp, 2005 Vail Hedberg Conference. AAPG Hedberg Series, 2008, No. 3, p. 87—104.

Jia C.Z., Wei G.Q., Li B.L. Yanshanian tectonic features in west-central China and their petroleum geological significance // Oil Gas Geol., 2005, v. 26(1), p. 9—15.

Law B.E. Basin-centered gas systems // AAPG Bull., 2002, v. 86(11), p. 1891—1919.

Law B.E., Curtis J.B. Introduction to unconventional petroleum systems // AAPG Bull., 2002, v. 86(11), p. 1851—1852.

Law B.E., Dickinson W.W. Conceptual model for origin of abnormally pressured gas accumulation in low-permeability reservoirs // AAPG Bull., 1985, v. 69(8), p. 1295—1304.

Li X.Q., Fen, S.B., Li J., Wang M., Huang X.B., Wang K.D., Kong L.X. Geochemistry of natural gas accumulation in Sulige large gas field in Ordos Basin // Acta Petrol. Sin., 2012, v. 28(3) , p. 836—846.

Liu X.S., Xi S.L., Fu J., Wang T., Wang X. Natural gas generation in the upper Paleozoic in E'erduosi basin // Nat. Gas Industry, 2000, v. 20(6), p. 19—23.

Meckel L.D., Thomasson M.R. Pervasive tight-gas sandstone reservoirs: An overview // Understanding, exploring, and developing tight-gas sands / Eds. S.P. Cumella, K.W. Shanley, W.K. Camp, 2005 Vail Hedberg Conference. AAPG Hedberg Series, 2008, No. 3, p. 13–27.

Meissner F.F. Causes of anomalous deep basin fluid pressures in Rocky Mountain basins and their relation to regional gas accumulation // 2000 Basin-Centered Gas Symposium: Rocky Mountain Association of Geologists, 2000, 11 p.

Nan J., Xie L., Liu S. The contributing factors of lower porosity and permeability reservoir in Permian in Sulige gas-field, Ordos Basin // J. Northwest University, 2005, v. 35(2), p. 207—211.

Nelson P.H. Pore-throat sizes in sandstones, tight sandstones, and shales. AAPG Bull., 2009, v. 3(93), p. 329—340.

Ren Z.L. Thermal history of Ordos basin assessed by apatite fission track analysis // ACTA Geophys. Sin., 1995, v. 38(3), p. 339—349.

Schmoker J.W. Resource-assessment perspectives for unconventional gas systems // AAPG Bull., 2002, v. 86(11), p. 1993—1999.

Shanley K.W., Cluff R.M., Robinson J.W. Factors controlling prolific gas production from low-permeability sandstone reservoirs: Implications for resource assessment, prospect development, and risk analysis // AAPG Bull., 2004, v. 88(8), p. 1083—1121.

Spencer C.W. Hydrocarbon generation as a mechanism for overpressuring in Rocky Mountain region // AAPG Bull., 1987, v. 71(4), p. 368—388.

Xiao X.M., Zhao B.Q., Thu Z.L., Song Z.G., Wilkins R.W.T. Upper Paleozoic petroleum system, Ordos Basin, China // Mar. Pet. Geol., 2005, v. 22(8), p. 945—963.

Xie Q.B., Sun J., Chen Q.P. Model of the distribution of the polygenetic channel sand body of Sulige large gas field // Earth Sci. Front., 2013, v. 20(2), p. 40-51.

Xu H., Tang D.Z., Zhang J.F., Yin W., Zhang W.Z., Lin W.J. Factors affecting the development of the pressure differential in upper Paleozoic gas reservoirs in the Sulige and Yulin areas of the Ordos Basin, China // Int. J. Coal Geol., 2011, v. 85(1), p. 103—111.

Yang H., Fu J.H., Liu X.S., Fan L. Formation conditions and exploration technology of large-scale tight sandstone gas reservoir in Sulige // Acta Petrol. Sin., 2012, v. 33(s1), p. 27—36.

Yang X.P., Zhao W.Z., Zou C.N., Li W., Tao S.Z. Comparison of formation conditions of "sweet point" reservoirs in Sulige gas field and Xiangxi Group gas field in the central Sichuan basin // Nat. Gas Industry, 2007, v. 27(1), p. 4—7.

Zhao M.W., Behr H.J. Vitrinite reflectance in Triassic with relation to geothermal history of Ordos basin // Acta Petrol. Sin., 1996, v. 17(2), p. 15—23.

Zhao W.Z., Wang Z.C., Zhu Y.X., Wang Z.Y., Wang P.Y., Liu X.S. Forming mechanism of low-efficiency gas reservoir in Sulige Gas Field of Ordos Basin // Acta Petrolei Sinica, 2005, v. 26(5), p. 5—9.

Zou C.N., Tao S.Z., Zhu R.K. Formation and distribution of "continuous" gas reservoirs and their giant gas province: A case from the Upper Triassic Xujiahe Formation giant gas province, Sichuan Basin // Petrol. Explor. Dev., 2009, v. 36(3), p. 307—319.

Zou C.N., Tao S.Z., Hou L.H., Zhu R., Yuan X.J., Song Y., et al. Unconventional petroleum geology // Beijing, Geology Press, 2013, 19 p.